



HAL
open science

Friction Laws for Saturated/Unsaturated Fatty Acid Layers

Fadlallah Abouhadid, Alexia Crespo, Nazario Morgado, Denis Mazuyer, Juliette Cayer-Barrioz

► **To cite this version:**

Fadlallah Abouhadid, Alexia Crespo, Nazario Morgado, Denis Mazuyer, Juliette Cayer-Barrioz. Friction Laws for Saturated/Unsaturated Fatty Acid Layers. Tribology Letters, 2021, 69, pp.46. 10.1007/s11249-021-01419-9 . hal-03255680

HAL Id: hal-03255680

<https://hal.science/hal-03255680>

Submitted on 9 Jun 2021

HAL is a multi-disciplinary open access archive for the deposit and dissemination of scientific research documents, whether they are published or not. The documents may come from teaching and research institutions in France or abroad, or from public or private research centers.

L'archive ouverte pluridisciplinaire **HAL**, est destinée au dépôt et à la diffusion de documents scientifiques de niveau recherche, publiés ou non, émanant des établissements d'enseignement et de recherche français ou étrangers, des laboratoires publics ou privés.

[Click here to view linked References](#)

Friction Laws for Saturated/Unsaturated Fatty Acid Layers

Special issue dedicated to the Memory of Mark Robbins

Fadlallah Abouhadid, Alexia Crespo, Nazario Morgado, Denis Mazuyer

*and Juliette Cayer-Barrioz**

Laboratoire de Tribologie et Dynamique des Systèmes, CNRS UMR5513, Ecole centrale de

Lyon, 36 avenue Guy de Collongue, 69134 Ecully cedex, France

Email: juliette.cayer-barrioz@ec-lyon.fr

Author ORCIDs:

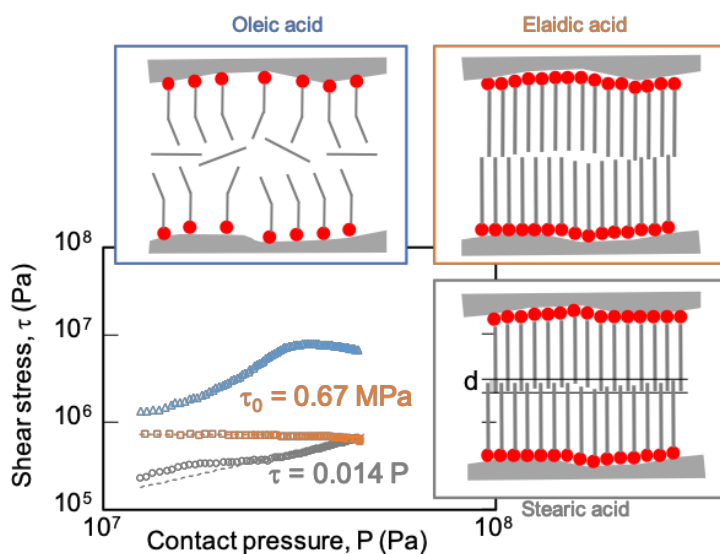
Denis Mazuyer: 0000-0001-9828-6884

Juliette Cayer-Barrioz: 0000-0002-3601-2957

Abstract

The presence or absence of unsaturation in the carbon chain of carboxylic acids was examined on the friction response of boundary films according to normal force. Friction laws were established as a function of the normal force at the nanoscale with a molecular tribometer derived from a surface force apparatus. While the shear plane is mainly composed of methyl groups in all the cases investigated, the molecular organization differs within the shear plane, as suggested by the simultaneous film thickness evolution. This gave rise to dissipation modes within the interface, resulting in a wide range of shear stress levels and dependence with contact pressure. The friction laws were discussed, highlighting the combined role of nanometric surface roughness and molecule unsaturation.

Graphical Abstract



Friction laws for stearic acid (\circ), elaidic acid (\square) and oleic acid (\triangle) boundary layers and schematic diagrams of the corresponding sheared interfaces

Keywords: Boundary lubrication, Friction modifiers, Molecular organization, Nanotribology, Surface force apparatus

Declarations: Not applicable

Funding: This work was supported by the Agence Nationale de la Recherche via the project Confluence ANR-13-JS09-0016-01 and by the LABEX Manutech-Sise (ANR-10-LABX-0075) of Université de Lyon, within the program “Investissements d’Avenir” (ANR-11-IDEX-0007) operated by the French National Research Agency (ANR), via the project DysCo. Additional support was also provided by the Agency for the ecological transition ADEME through the IMOTEP project.

Conflicts of interest: The authors have no conflicts of interest to declare

1
2 **Availability of data and material:** Supporting Information is available from the corresponding
3
4 author, JCB, upon reasonable request.
5
6

7
8
9 **Authors' contributions:** JCB designed the study and wrote the initial version of the manuscript.
10
11 Data collection and analysis was performed by AC, FA, NM and JCB. The theoretical model
12
13 was developed by DM. Manuscript editing and revisions were performed by FA, NM, DM and
14
15 JCB.
16
17
18
19
20
21
22
23
24
25
26
27
28
29
30
31
32
33
34
35
36
37
38
39
40
41
42
43
44
45
46
47
48
49
50
51
52
53
54
55
56
57
58
59
60
61
62
63
64
65

1. Introduction

Early experiments and theories by Leonardo da Vinci, Amontons, Coulomb, Archard, Bowden and Tabor, and others established friction laws at the macroscale in multi-asperity contacts [1].

Amontons, in 1699 and then, Coulomb in 1781, thus proposed the first friction laws between sliding solid surfaces in contact and the dependence with sliding velocity, normal load, apparent contact area and halting time before sliding [2]. Two centuries later, Bowden and Tabor physically interpreted solid friction taking into account the mechanical properties of the solids and the surface roughness. The real contact area of a multi-asperity contact was smaller than the apparent contact area, giving rise to the formation of plastic cohesive junctions that needed to be sheared to slide. These authors introduced the concept of interfacial shear stress as the ratio between the friction force and the real contact area.

At the nanoscale, the variation of friction with the normal force are still under scrutiny according to the contact roughness, the nature of the surfaces, the presence of a lubricant, etc [2-14]. For instance, for dry contacts, Luan et al. [8] modelled a sublinear dependence of friction with the load while Gao et al. [9] predicted a linear variation. The existence of these two laws and the transition from sublinear to linear dependence was later attributed to the surface roughness, in regard with the range of interfacial interactions [10]. The adhesion contribution, responsible for the sublinear law, was found proportional to the number of interatomic bonds, continuously broken and reformed during sliding [9]. For lubricated contacts, surface films were often modeled as self-assembled films, made of vertically attached molecules via their polar groups. The van de Waals forces between the end groups of these molecules lead to a weakly adhesive interface, where the shear plane is localized, and cause boundary friction [11]. Briscoe et al. [12] analyzed the evolution of shear stress of Langmuir-Blodgett films of calcium stearate with pressure. He showed that a transition occurred with contact pressure: at low contact

1
2
3
4
5
6
7
8
9
10
11
12
13
14
15
16
17
18
19
20
21
22
23
24
25
26
27
28
29
30
31
32
33
34
35
36
37
38
39
40
41
42
43
44
45
46
47
48
49
50
51
52
53
54
55
56
57
58
59
60
61
62
63
64
65

pressure, the shear stress was constant while it increased in proportion with the pressure for contact pressures greater than 50 MPa [12]. The existence of a contact pressure transition was later observed by Ruths et al. [13]. The effect of pressure was explained by an increasing squeeze of the molecular chains and thus an increasing sliding force [12].

Briscoe et al. [12] also showed this general pattern for various types of confined interfaces, restating the question of the dependence of the friction force of hydrocarbon materials with the structure or orientation of the molecules. Nevertheless, Homola et al. [14] showed that the value of the constant shear stress depended on the number of layers of OMCTS trapped between mica surfaces. When loose-packed monolayers made of alkane molecules co-adsorbed with carboxylic acids and separated by squalane, hexadecane or more viscous polyalphaolefin, were sheared, a linear increase in friction force with the normal force was measured, regardless of the contact pressure [15-17]. The solvent separating opposite monolayers also play a role: a low pull-off force was measured in larger dielectric constant solvent and was associated to a Amontons-like linear friction evolution with normal force [13, 18].

Sutcliffe et al. also advanced a theory describing friction with a two-term relation [11]. As surfaces relatively move, the first term corresponds to an interaction energy barrier encountered from one equilibrium position to the next equilibrium position, as well as the work done against rotation energy barriers, while the second term represents the energy required to lift one end group over the opposite. In this model, the terminal groups only were considered capable of internal rotations and deformations. The role of the terminal groups in friction was also supported by Colburn et al. [18] and Frisbie et al. [19] who showed that shearing a CH₃/CH₃ interface required more energy dissipation than a CH₃/COOH interface, for instance.

This brief literature review highlighted the co-existence of different friction laws in boundary friction depending on the contact pressure, the nature of the functional groups, the effect of the solvent, etc. In this work, to elucidate the friction mechanisms and identify the role of the

1 localization of the shear plane related to the molecular organization, regardless of the
2 environment, of the chain length and of the surface roughness, 18-carbon chain fatty acids were
3 selected with/without unsaturation. When present, the unsaturation was either in cis or in trans
4 configuration. We experimentally established friction laws at the nanoscale, over three decades
5 of normal force, and explored the correlation between friction laws, molecular organization and
6 properties of the confined layers. The self-assembled layers that were rubbed, were formed from
7 a dilute solution of saturated/unsaturated fatty acids in dodecane used as solvent.
8
9
10
11
12
13
14
15
16
17
18

19 **2. Experimental Section**

20 *2.1. Liquids*

21 Highly pure (>99.0%) molecules were purchased from Sigma Aldrich. Before use, dodecane
22 was dehydrated with zeolites for several days and filtrated using a 200 nm nucleopore filter.
23 Dodecane molecule has an estimated diameter of 4 Å for a length, L_0 , of 14 Å. Low
24 concentration solutions of fatty acids (stearic, elaidic and oleic acids) in dodecane were
25 prepared at 2 mM to maintain the viscosity unchanged at 1.5 mPa.s at 23°C. Stearic acid
26 molecule has a saturated straight alkyl chain with 18 carbons and its estimated length, L_0 , is
27 21.4 Å [20]. Elaidic and oleic acids are mono-unsaturated with a double carbon bond in ω9,
28 either in trans or cis configuration. Elaidic acid chain remain straight with an estimated length,
29 L_0 , of 21.2 Å while oleic acid chain is bent with an estimated length, L_0 , of 19.25 Å [20].
30
31
32
33
34
35
36
37
38
39
40
41
42
43
44
45
46
47
48
49

50 *2.2. Surfaces*

51 The sphere was made of fused silicate glass. The radius of each sphere was systematically
52 measured five times, after the experiment using both Bruker interferometry profilometer and a
53 caliper, with a resolution of ± 0.05 mm. The radius values are indicated in Table 1.
54
55
56
57
58
59
60
61
62
63
64
65

Table 1. Radii of the cobalt-coated fused silicate glass spheres

Experiment	Dodecane	Stearic acid solution	Elaidic acid solution	Oleic acid solution
Radius, R ($\times 10^{-3}$ m)	2.10 ± 0.05	2.03 ± 0.05	1.94 ± 0.05	2.00 ± 0.05

The plane was made of <100> silicon wafer and was initially cleaned with isopropanol and deionized water using a spin-coater at 8000 tr/min and then dried under Nitrogen flow before coating deposition. In order to mimic metallic surfaces and to make the sphere/plane pair chemically symmetrical, a 40 nm thin Cobalt coating was deposited on each surface, using cathodic sputtering under low argon pressure at 10^{-6} mbar [21]. XPS analysis confirmed the existence of a 0.3 nm thin oxide layer [22]. Multi-scale topography analysis was performed before and after the experiment using Brüker interferometry profilometer in Phase Shift Interferometry mode, over $63 \times 47 \mu\text{m}^2$, providing a root mean square roughness, S_q , of 0.5 nm on both surfaces. This low roughness value was also confirmed on the cobalt-coated plane using AFM over $1 \times 1 \mu\text{m}^2$, with $S_q = 0.3$ nm. No surface damage was observed after the experiment.

2.3. Friction using the ATLAS molecular tribometer

This apparatus was described in detail by Tonck et al. [23]. and Crespo et al. [21]. In these experiments, the use of electrical measurement of the metallic sphere/plane capacitance allowed us to define the absolute zero separation distance [21]. The environment temperature was 23 ± 0.5 °C and the atmosphere was kept dry ($< 2\%$ RH) with argon at ambient pressure. The cleanliness of the contact was checked before the actual experiments as no repulsive force was detected between the two surfaces, down to few nm of separation. A droplet of solution was then deposited between the two surfaces. After few hours, in order to reach full and stable adsorption of the fatty acids on the surfaces, “landing” friction experiments were performed: the sliding velocity, V_x , was equal to 1.0 nm/s for the dodecane and the stearic acid solution,

1 and to 1.5 nm/s for the elaidic and oleic acid solutions, and the approaching velocity, V_z , was
2 0.1 nm/s. The ratio, V_x/V_z , was maintained larger than 10 with a very low V_z in order to ensure
3 steady-state friction and to decrease the squeeze contribution of the fluid. The normal and
4 friction forces, respectively F_z and F_x , were simultaneously and independently measured with
5 a resolution better than 1 μN [21]. In parallel, dynamic measurements were performed in the x-
6 direction with an oscillation amplitude of ± 0.05 nm at a frequency f_x of 70 Hz, providing the
7 elastic stiffness K_x and the viscous damping, $A_x \cdot 2\pi f_x$, of the interface [21]. When surfaces come
8 into contact, the normal force increases, inducing the sphere deformation, according to Hertz
9 theory in absence of adhesion or Derjaguin-Muller-Toporov (DMT) theory in the presence of
10 adhesion [24]. Taking into account this solid deformation allowed us to calculate the real
11 surface separation, D , assuming the confined interface is much stiffer than the sphere/plane
12 contact. This assumption was based on the values of contact pressure [25], here about and above
13 20 MPa, and on the rather high coverage ratio of the molecules on the surfaces (as confirmed
14 by [24] for similar surfaces and molecules).
15
16
17
18
19
20
21
22
23
24
25
26
27
28
29
30
31
32
33

37 **3. Results and Discussion**

38 *3.1. Friction of dodecane interface*

39
40
41 The friction response of dodecane to an increase of the confinement, is presented in Figure 1.
42
43 The friction force was proportional to the normal force, meaning that a friction coefficient can
44 be defined as the slope of the curve. The friction coefficient was 0.45, a rather high value, but
45 in good agreement with previous findings [26]. The friction force obeys Amontons-Coulomb
46 law [27].
47
48
49
50
51
52
53
54
55
56
57
58
59
60
61
62
63
64
65

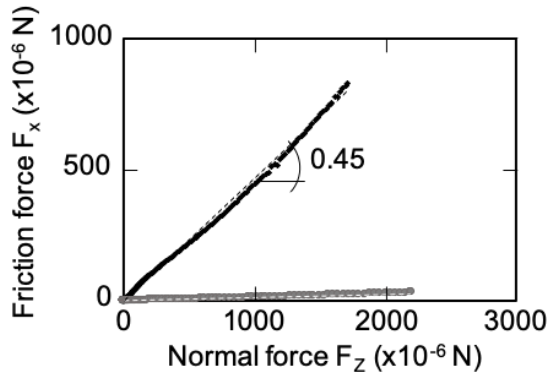


Figure 1. Linear evolution of the friction force as a function of the normal force for confined dodecane (\diamond) with a slope of 0.45. The low friction force measured for the stearic acid solution (\circ) was also indicated as a sake of comparison.

In parallel, the separation distance between the deformed sphere and the plane, corresponding to the dodecane film thickness, was plotted in Figure 2. Two stages were observed: first, at the onset of increase of the normal force, the dodecane film thickness strongly decreased; second, from a normal force ranging from 350 to 1700 μN , the film thickness decreased more slowly, from 47 to 10 \AA , obeying the trend in Equation 1:

$$D(F_z) = -a \cdot F_z + b \quad (1)$$

with $a^{-1} = 3.7 \cdot 10^5 \text{ N/m}$ and $b = 57 \text{ \AA}$. This linear decreasing trend was observed with squalane in [9]. In addition, the inverse value of the slope, corresponding to a stiffness in terms of unit, was consistent with the normal stiffness of the dodecane layer, i.e. its elasticity [2].

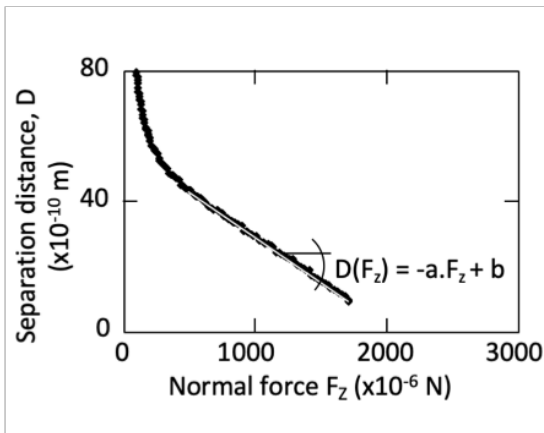


Figure 2. Associated variation of the sphere/plane separation distance, D , for dodecane (\diamond). A linear decrease in the distance as the normal force increased from 350 to 1700 μN , was observed, from 47 \AA down to 10 \AA , meaning that many layers of dodecane separated the two surfaces. $a=0.027 \text{ \AA}/\mu\text{N}$ and $b = 57 \text{ \AA}$.

1
2 The transition between these two stages occurred for a Hertzian contact radius, a_H , of 2 μm ,
3
4 which corresponds to the load from which a rather “stable” elastic wall of dodecane was
5
6 squeezed in the contact due to the molecule confinement. This wall remained thick compared
7
8 to the size of the molecule, L_0 . Molecular dynamic experiments from Jabbarzadeh et al. [28]
9
10 and Cui et al. [29] pictured dodecane adsorbed parallel to atomically smooth mica surfaces. In
11
12 a first approximation, it could then be assumed the dodecane layer was sheared in a
13
14 homogeneous viscous manner. The theoretical viscous friction force for piezoviscous dodecane
15
16 was calculated as:
17
18

$$19 \quad F_x = \frac{\eta_0 \cdot e^{\alpha \cdot P} \cdot V_x}{D} \cdot \pi a_H^2 \quad (2)$$

20
21 with the viscosity $\eta_0 = 1.5 \text{ mPa}\cdot\text{s}$, the pressure-viscosity coefficient $\alpha = 22 \text{ GPa}^{-1}$, the sliding
22
23 velocity $V_x = 1 \text{ nm/s}$, the contact pressure P and the contact radius a_H . Thus, assuming a viscous
24
25 dissipation, the theoretical friction force should not increase linearly with the normal force since
26
27 a_H^2 increases as $F_z^{2/3}$ and D roughly decreases as F_z . In addition, the calculated friction force
28
29 was of the order of magnitude of 10^{-13} N , inconsistent with the values measured in Figure 1.
30
31 This seems to indicate that the shear of dodecane was either heterogeneous, or non-viscous or
32
33 both, regardless of the normal force applied. In this work, rms roughness amplitude was larger
34
35 than in the work of Jabbarzadeh et al. [28] and Cui et al. [29]. Here, the wavelength of the
36
37 roughness was over 1 μm , meaning that at the scale of the dodecane molecule, the surfaces
38
39 could be considered as relatively smooth. However, this long-wavelength perturbation could
40
41 lead to disorganized stacking of dodecane molecules which cannot be mainly aligned as
42
43 suggested in the literature. This could explain the high level of the friction force with shear
44
45 mechanisms remaining similar, regardless of the dodecane film thickness down to 10 \AA . The
46
47 absence of adhesion term in the dodecane friction force could also be explained by this thick
48
49 film.
50
51
52
53
54
55
56
57
58
59
60
61
62
63
64
65

3.2 Friction with fatty acid boundary layers

A dramatic change in friction behavior resulted from the addition of a polar carboxylic anchor to the alkyl chain as the level of friction force decreased by one or two orders of magnitude (see Figure 1, 3a and 3b).

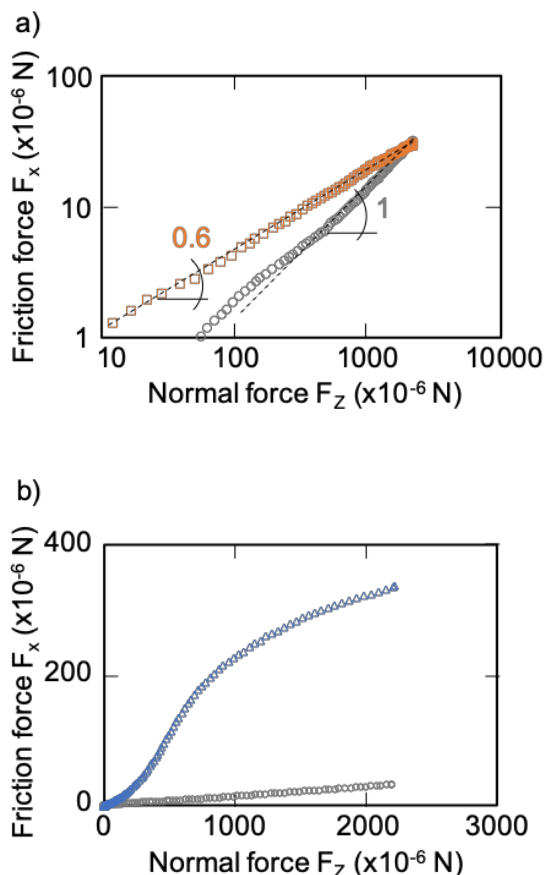
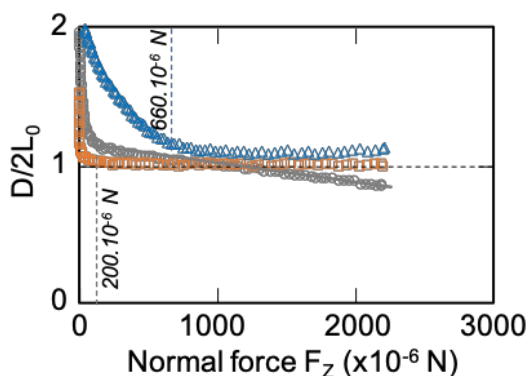


Figure 3. Influence of the molecular architecture on the friction force variation for fatty acids (a) for the straight alkyl chain, stearic acid (\circ) and elaidic acid (\square) in logarithmic scale, and (b) for the bent alkyl chain oleic acid (\triangle) in linear scale. The stearic acid data were also reported in (b) for sake of comparison.

Above normal forces of 200 μ N, the stearic acid friction force increased roughly linearly with the normal force, quasi following Amontons-Coulomb law with a friction coefficient of 0.014 and no adhesive term. The evolution of the friction force was very similar to that observed with dodecane. However, the level of friction was significantly decreased compared to the dodecane case, exhibiting quasi-superlubricity. The absence of adhesive term, i.e. $F_x = 0$ for $F_z = 0$ for all

1 the molecules, was consistent with previous pure squeeze measurements [24]. In presence of
 2 unsaturation, the friction force variation completely differed: the elaidic acid friction force
 3 varied as $(F_z)^{0.6}$ and the oleic acid friction force increased non-linearly with the normal force,
 4 in a very complex manner, as shown in Figure 3a and 3b.
 5
 6
 7
 8
 9

10
 11 The analysis of the associated evolution of the film thickness shed light into the possible
 12 interface configuration and shear mechanisms. Figure 4 shows that a plateau of film thickness
 13 was reached for differing normal forces, depending on the fatty acid.
 14
 15
 16
 17
 18
 19



20
 21
 22
 23
 24
 25
 26
 27
 28
 29
 30
 31
 32
 33 **Figure 4.** Dimensionless film thickness evolution, $D/2L_0$, with increasing confinement for
 34 stearic acid (○), elaidic acid (□) and oleic acid (△). A thickness plateau was more or less
 35 reached for the three fatty acids at about 42 Å. The theoretical thickness of two layers of vertical
 36 molecules, $2L_0$, was used to calculate the dimensionless film thickness for each molecule.
 37
 38

39
 40 The existence of such a difference with dodecane behavior was expected as adsorption of fatty
 41 acids on the metallic surfaces was likely due to the strong interactions between the polar group
 42 and the cobalt oxides [24, 30]. However, the film thickness also varied with the
 43 presence/absence of unsaturation. In the case of stearic acid, the onset of increase in normal
 44 force was detected from a film thickness of 54 Å, larger than $2L_0$ with L_0 the estimated length
 45 of the molecule, meaning a dodecane layer whose thickness is 10 Å could be trapped between
 46 the stearic acid layers, assuming the stearic acids vertically adsorbed on the surfaces. The
 47 dodecane trapping could be due to the stearic acid organization on the surfaces as discussed
 48 later. From 200 μN (and 48 Å), the film thickness slightly decreased of about 10 Å linearly as
 49
 50
 51
 52
 53
 54
 55
 56
 57
 58
 59
 60
 61
 62
 63
 64
 65

1
2
3
4
5
6
7
8
9
10
11
12
13
14
15
16
17
18
19
20
21
22
23
24
25
26
27
28
29
30
31
32
33
34
35
36
37
38
39
40
41
42
43
44
45
46
47
48
49
50
51
52
53
54
55
56
57
58
59
60
61
62
63
64
65

the normal force increased. This could suggest that the fatty acid molecules were not highly packed in the layers which leads to a higher compliance than for complete monolayers. This compliance was not initially taken into account in the estimation of sphere/plane distance as the contact pressure was high, here above 15 MPa, and that the surface coverage was also large. At 2200 μN , the film thickness reached 38 \AA , smaller than $2L_0$: this could confirm the interpenetration process between the stearic acid layers (see Figure 5 a-i and b-i). However, this interpenetration zone would remain thin with a thickness of 4 \AA at the highest normal force and could involve the terminal methyl groups. Another description would consist in considering a mixed layer of dodecane and stearic acid, as seen by Ruths et al. [13]. Nevertheless, we measured a smaller friction, indicating that the molecular structure could presumably differ and that the effect of dodecane is not dominant.

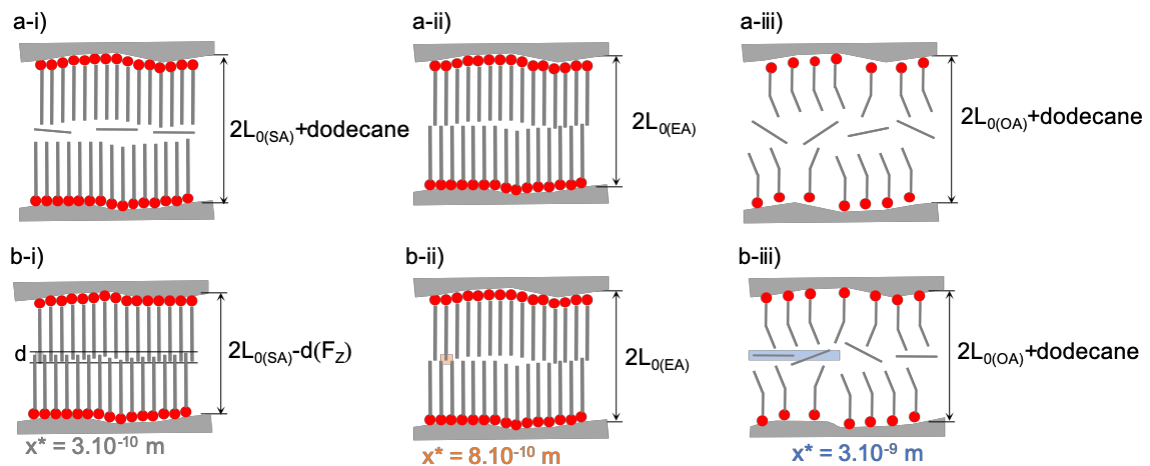


Figure 5. Schematic of the interface configuration as a function of the normal force, (a) at low normal force and (b) at higher normal force, $F_z > 600 \cdot 10^{-6} \text{ N}$, for stearic acid (i), elaidic acid (ii) and oleic acid (iii) at the scale 1:1. The values of threshold distance, x^* , measured independently, were indicated at the interface, using a colored rectangle.

Elaidic acid (with one trans-unsaturation) stabilized film thickness corresponds to twice the length of the molecule, $2L_0 = 42 \text{ \AA}$. This value was reached at low normal force, indicating that one layer of elaidic acid was vertically adsorbed on each surface. The fact that the film thickness did not depend on the normal force suggests that the monolayers were rather dense and stiff, limiting the interpenetration between monolayers. This was consistent with the molecular

1 organization description proposed by Crespo et al. [24] who showed the role of the hydrocarbon
2 chain on the steric hindrance and molecular organization. The area occupied per molecule could
3 then be estimated at about $20\text{-}22 \times 10^{-20} \text{ m}^2$ [24]. A schematic was presented in Figure 5 a-ii and
4 b-ii to illustrate this interface configuration.
5
6
7
8

9
10 The presence of the unsaturation in cis configuration lead to a bent shape of the oleic acid
11 molecule and a smaller length, L_0 . Under confinement, the film thickness measured for oleic
12 acid decreased slowly as the normal force increased up to $660 \mu\text{N}$ and then reached a plateau,
13 corresponding to twice the length, $2L_0$, and to a layer of dodecane entrapped between these
14 layers. The dodecane structuring over the oleic acid layers clearly contributed to the forming of
15 a confined layer: the bent shape of the oleic acid and the low coverage ratio ranging from 25
16 and $50 \times 10^{-20} \text{ m}^2$ mentioned in the literature [24, 31] seemed to favor the presence of a dodecane
17 layer, that got entrapped during the confinement, as illustrated in Figure 5 a-iii and b-iii.
18
19
20
21
22
23
24
25
26
27
28
29
30
31

32 A classical steady-state friction curve vs sliding distance is usually described by a linear
33 increase phase characterized by its slope, the elastic stiffness, K_x , followed by a friction force
34 plateau at a limited value F_{xl} [32]. The transition between these two periods occurs for a sliding
35 distance, x^* , defined by:
36
37
38
39
40

$$41 \quad x^* = F_{xl}/K_x \quad (3)$$

42
43 This distance corresponds to the sliding distance beyond which the steady-state regime is
44 reached [33]. The tangential elastic stiffness, K_x , was measured independently during a “landing”
45 friction experiment. K_x varied with the normal force. Nevertheless, $K_x(\text{elaidic acid}) < K_x(\text{stearic}$
46 acid) $\ll K_x(\text{oleic acid}) \approx K_x(\text{dodecane})$, The calculated threshold distance, x^* , was plotted as a
47 function of the normal force in Figure 6 for the stearic, elaidic and oleic acid solutions. This
48 distance was independent of the normal force and considered as a signature of the interface
49 depending on the fatty acid: it increased from 3 \AA , 8 \AA to 30 \AA respectively for stearic acid,
50
51
52
53
54
55
56
57
58
59
60
61
62
63
64
65

elaïdic acid and oleïc acid. This distance was also reported on Figure 5. Interestingly (but likely a coincidence), it has the same order of magnitude as the lateral distance between the chain ends in the interpenetration zone for the stearic acid, as the lateral distance between the chains at the interface between the two elaïdic acid monolayers and as the length of dodecane molecules entrapped between the two oleïc acid monolayers.

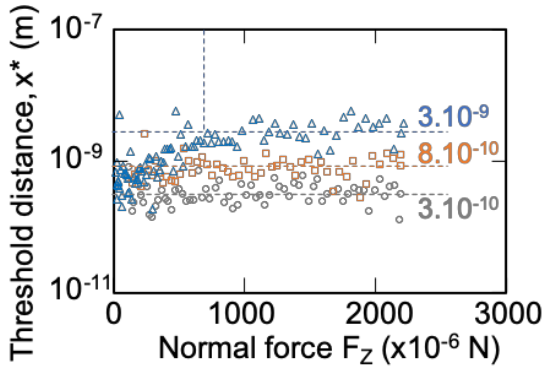


Figure 6. Threshold distance, x^* , calculated using Equation 3 vs the normal force, F_z , for stearic acid (\circ), elaïdic acid (\square) and oleïc acid (\triangle). A plateau was rapidly reached for the stearic acid and the elaïdic acid at 3 Å and 8 Å respectively. In the case of oleïc acid, this distance x^* increased to finally reach 30 Å at high normal force.

3.3. Discussion

The following discussion was restricted to loads higher than the loads at which distance D reaches $2L_0$, when the studied interfaces were considered as fully confined and “steady-state” regimes were reached.

The surfaces were assumed to be rough and covered by a more or less compact monolayer of fatty acids with an area occupied by a molecule, a_{eff} . This means that the loaded surfaces interact over a real contact area, A_r , by making junctions inside which the monolayers may interpenetrate through a distance, d , as shown in Figure 5. According to Tabor adhesion theory, the friction force, F_x , could then be written as:

$$F_x = \tau_s \cdot A_r \quad (4)$$

where τ_s was the mean interfacial shear stress of a junction. When fully-confined, the interface was supposed to behave as a rigid wall, the real contact area was given by the solid elasticity

1 and could be described by the Greenwood-Williamson theory [34]. This means that the
2 observed thickness variation originated either from elastic deformation of the asperity summits
3 or from the capability of the layers to interpenetrate. Then the contribution of each of them
4 depend both on the number of chains per unit area (l/a_{eff}) and on their flexibility i.e. the presence
5 or not of unsaturation. The interfacial shear strength was supposed to depend only on the way
6 the molecules interpenetrate inside a junction. The adsorption model proposed by [35] and [36]
7 for grafted polymer chains was then used to describe the evolution of the tangential stress with
8 the contact pressure. This model supposed that the interdigitation process between two grafted
9 layers with a thickness, L_0 , is similar to the adsorption of a molten brush onto a solid surface by
10 the free end points of the chains (see Figure 7). The fraction of interpenetrated chains which
11 form a bridge with the opposite layer inside one junction is called η . When two adsorbed layers
12 were loaded together and sheared against each other, they formed junctions in which the
13 molecules can interdigitate through the thickness d . Three types of junctions that could be
14 sheared together inside the apparent Hertzian contact area were distinguished.

- 15 • The first one corresponded to the case when during sliding, all the fatty acid chains
16 made bridging inside one junction ($\eta \approx 1$) from one surface to the other. Thus, the
17 thickness d of the interpenetration zone is close to 0 and the cobblestone model [37] can
18 be applied resulting in a strength of the junction τ_l independent of the load. Its
19 contribution concerns a total area A_1 .
- 20 • The second one corresponded to junctions in which only a fraction $\eta < 1$ of fatty acid
21 chains made bridging. Then due to shearing, the chains forming bridges were stretched
22 further and the fraction of bridges decreased. For a critical value, η_c , of the latter, the
23 force reached a maximum value and the system became mechanically unstable, leading
24 to sliding. Its contribution to the whole interfacial stress was called τ_2 and concerned a
25 total area A_2 .

- The third one corresponded to confined layers of dodecane molecules trapped between the two adsorbed fatty acid monolayers. Its contribution to the whole interfacial shear stress was called τ_3 and concerned a total area A_3 . Then we got,

$$A_1 + A_2 + A_3 = A_H, \quad (5)$$

$$A_1 + A_2 = A_r, \quad (6)$$

and

$$F_x = \tau_1.A_1 + \tau_2.A_2 + \tau_3.A_3 \quad (7)$$

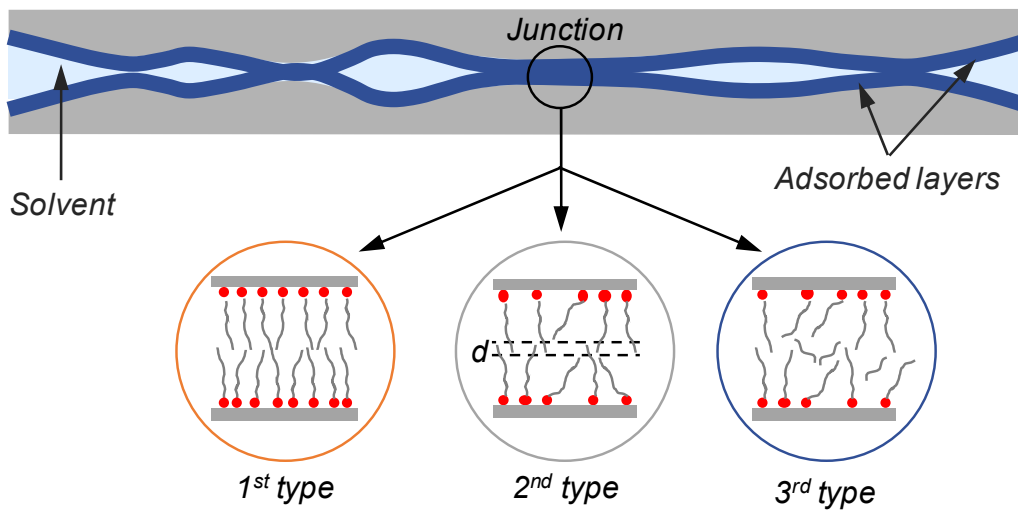


Figure 7. Schematic diagram presenting the sheared interface and the three types of junctions.

3.3.1. Elaidic acid friction

The experimental results suggest that the frictional force is mainly given by the first type of junctions, which enables us to neglect the contribution of τ_2 and τ_3 . Because of the straight shape of the elaidic acid molecule, the model, referred to as the cobblestone model [37] and applied to one junction seemed to perfectly account for the friction law observed for elaidic acid. The friction was originated from the pressure dominated by van der Waals forces rather than the applied load. The shear plane was localized at the interface between the two monolayers. The dissipated energy due to junction shearing was a fraction of the adhesive work, resulting in a

constant shear stress, independent of the normal force. This interfacial shear stress, τ_l , could be calculated from the surface energy between methyl groups, here $2 \cdot \gamma \cdot a_{eff} \sim 10^{-20}$ J with $\gamma = 22$ mJ.m⁻² and a_{eff} the effective area of elaidic molecular groups, here $a_{eff} = 20 \times 10^{-20}$ m², and from a fraction of energy usually equal to 1/30 [25, 38-39]. This would lead to a theoretical interfacial shear stress $\tau_l = 3.3$ MPa for one junction. Supposing the number of contact spots, n , is given by the Greenwood-Williamson theory, it is shown that, for an exponential distribution of height asperities, $n \sim \exp(-D/\sigma)$, where σ is the rms roughness of the surfaces.

As D is independent of the normal load F_z , the real contact A_r is such as $A_r \sim \exp(-D/\sigma) \cdot F_z^{2/3}$.

Then, $F_x \sim \exp(-D/\sigma) \cdot \tau_l \cdot F_z^{2/3}$, consistent with our observations.

This also showed that the interfacial stress is constant for elaidic acid layers. In addition, as $D \gg \sigma$, this means that $\exp(-D/\sigma)$ is much lower than 1, explaining why the measured interfacial shear strength is much lower than the one that would be calculated if the surfaces were smooth.

3.3.2. Stearic acid friction

The slight decrease in interface thickness observed with stearic acid molecules and their higher flexibility, suggested the second type of junctions mainly contributed to the frictional force. In this assumption framework, the lubrication model of [35] and [36] based on the capability of stearic acid monolayers to interdigitate during squeeze and shearing could be applied.

Assuming the interdigitation thickness is small compared to the length of the molecule, it gave the following results: $\eta_c \sim \delta^{1/3} \cdot a_{eff} \cdot P_s^{1/2}$, $d \sim a_{eff} \cdot P_s^{1/2}$ and $\tau_s \sim \delta^{5/6} \cdot a_{eff} \cdot P_s^{1/2}$, where τ_s (resp. P_s) are the interfacial shear stress of one junction (resp. the pressure borne by one junction) and δ is a non-dimensional adhesion energy between two fatty acid molecules. The evolution of the friction force F_x with normal force F_z was then dependent on the model used to describe the real contact area A_r . If the contact is considered as Hertzian, then $F_x \sim F_z^{5/6}$ and d increases as $F_z^{1/6}$. If A_r is given by the Greenwood model, then $F_x \sim F_z$ and d is constant as well as distance

1
2
3
4
5
6
7
8
9
10
11
12
13
14
15
16
17
18
19
20
21
22
23
24
25
26
27
28
29
30
31
32
33
34
35
36
37
38
39
40
41
42
43
44
45
46
47
48
49
50
51
52
53
54
55
56
57
58
59
60
61
62
63
64
65

D since P_s is independent of the load. If A_r is given by Archard model [40], then $F_x \sim F_z^{17/18}$ and d scales as $F_z^{1/18}$ which means the sphere/plane distance slightly decreased with load. The comparison of this raw theoretical approach to the experimental results suggests that the Archard modelling of contact area seemed appropriate to catch the role of surface roughness in the friction behavior of stearic acid layer at molecular scale.

3.3.3. Oleic acid friction

By contrast, in the case of oleic acid, the friction behavior clearly differed. The friction level was very high, closer to that of dodecane, and the friction force did not obey any known friction law. The oleic acid did not withstand shear well as successive loading/unloading experiments revealed a disorganized interfacial structure. This was presumed to originate from the presence of a dodecane layer and of the unsaturation in cis configuration as a very similar friction behavior was observed with glyceryl oleate interface (unpublished work). This suggested that interface made by the confined oleic acid layers mainly consisted of the third type of junctions. The poor molecular packing could result in more modes of energy dissipation and thus to higher friction [41].

4. Conclusion

This tribological analysis of carboxylic acid boundary layers sliding against one another over three decades of normal force exhibited various behaviors and levels of friction, from superlubricity to high values. We showed that the absence or presence of unsaturation and its configuration combined to roughness effects govern the boundary layer organization and thus, the localization and nature of the shear plane. The friction level and its dependence to normal force, or contact pressure, could therefore be explained by supposing the contact between the fatty acids monolayers was made through junctions that have to be sheared during sliding.

1
2 The dependence of the shear stress on the contact pressure was investigated through a three-
3
4 term friction law that includes the contribution of three types of junctions:
5
6

- 7 • The first one was associated to the van der Waals interactions between methyl groups inside
8 a junction between two dense monolayers characterized by a constant shear strength and a
9 friction force that scales as $F_z^{2/3}$ all over the real contact area. This is the main shearing
10 component that was involved in the friction response of elaidic acid monolayers which are
11 dense and “rigid” (thanks to the presence of the double bond in trans configuration in the
12 elaidic acid molecule structure).
13
14 • The second one was associated to the interdigitation capability of monolayers inside a
15 junction. According to the contact area modeling, this lead to a friction force F_x scaling
16 roughly as F_z and a slight decrease in the sphere/plane distance, as observed experimentally
17 for stearic acid monolayers.
18
19 • The third one was associated to the shearing of a thin layer of solvent molecules that could
20 be trapped between the monolayers. This contribution is supposed to explain the frictional
21 behavior of a “disordered” and less compact layers of oleic acid.
22
23
24
25
26
27
28
29
30
31
32
33
34
35
36
37
38

39 The relative contributions of each term were discussed thanks to this theoretical approach. The
40 latter could explain the effect of saturation/unsaturation presence and that of the molecular
41 organization, issued from the simultaneous and independent film thickness and tangential
42 stiffness measurements to the frictional behavior of self-assembled fatty acids monolayers.
43
44
45
46
47
48
49
50

51 **Acknowledgements**

52 This article is in memory of Professor Mark Robbins.
53

54 This work was financed by the Agence Nationale de la Recherche via the project Confluence
55 project ANR-13-JS09-0016-01 and by the LABEX Manutech-Sise (ANR-10-LABX-0075) of
56
57
58
59
60
61
62
63
64
65

operated by the French National Research Agency (ANR), via the project DysCo. Additional support was also provided by the Agency for the ecological transition ADEME through the IMOTEP project.

References

- [1] Dowson, D. History of Tribology, Longman, London, UK (1979).
- [2] Crespo, A. : Compréhension de la tribologie de films limites : De l'organisation moléculaire à la réponse en friction. PhD Thesis, Ecole centrale de Lyon, France, 2017LYSEC21, June 2017.
- [3] He, G., Robbins, M.O.: Simulations of the kinetic friction due to adsorbed surface layers. Tribol. Lett. 2001, 10, 7-14.
- [4] He, G., Müser, M. H., Robbins, M. O.: Adsorbed layers and the origin of static friction. Science 1999, 284, 1650-1652.
- [5] Berman, A., Drummond, C., Israelachvili, J.: Amontons' law at the molecular level. Tribol. Lett. 1998, 4, 95-101.
- [6] Yoshizawa, H., Chen, Y.L., Israelachvili, J.: Fundamental mechanisms of interfacial friction. 1. Relation between adhesion and friction. J. Phys. Chem. 1993, 97, 4128-4140.
- [7] Wenning, L., Müser, M.: Friction laws for elastic nanoscale contacts. Europhysics Letters 2001, 54, 693-699.
- [8] Luan, B., Robbins, M.O.: The breakdown of continuum models for mechanical contacts. Nature 2005, 435, 929-932.
- [9] Gao, J., Luedtke, W. D., Gourdon, D., Ruths, M., Israelachvili, J., Landman, U.: Frictional Forces and Amontons' Law: From the Molecular to the Macroscopic Scale. J. Phys. Chem. B 2004, 108, 3410-3425.
- [10] Mo, Y., Turner, K.T., Szlufarska, I.: Friction laws at the nanoscale. Nature 2009, 457, 111-1119.

- 1
2
3
4
5
6
7
8
9
10
11
12
13
14
15
16
17
18
19
20
21
22
23
24
25
26
27
28
29
30
31
32
33
34
35
36
37
38
39
40
41
42
43
44
45
46
47
48
49
50
51
52
53
54
55
56
57
58
59
60
61
62
63
64
65
- [11] Sutcliffe, J., Taylor, S. R., Cameron, A.: Molecular asperity theory of boundary friction. *Wear* 1978, 51, 181-192.
- [12] Briscoe, B. J., Scruton, B., Willis, F. R. : The shear strength of thin lubricant films. *Proc. R. Soc. Lond.* 1973, A333, 99-114.
- [13] Ruths, M., Lundgren, S., Danerlöv, K., Persson, K.: Friction of Fatty Acids in Nanometer-Sized Contacts of Different Adhesive Strength. *Langmuir* 2008, 24, 1509-1516.
- [14] Homola, A. M., Israelachvili, J. N., Gee, M. L., McGuiggan, P. M.: Measurements of and Relation Between the Adhesion and Friction of Two Surfaces Separated by Molecularly Thin Liquid Films. *J. Tribol* 1989, 111, 675-682.
- [15] Lundgren, S. Ruths, M., Danerlöv, K., Persson, K.: Effects of unsaturation on film structure and friction of fatty acids in a model base oil. *J. Colloid Inter. Science* **2008**, 326, 530-6.
- [16] Doig, M., Warrens, C. P., Camp, P. J. : Structure and Friction of Stearic Acid and Oleic Acid Films Adsorbed on Iron Oxide Surfaces in Squalane. *Langmuir* 2014, 30, 186-195.
- [17] Yamada, S., Inomata, K. A., Kobayashi, E., Tanabe, T., Kurihara, K.: Effect of a Fatty Acid Additive on the Kinetic Friction and Stiction of Confined Liquid Lubricants. *Tribol. Lett.* 2016, 64, 23.
- [18] Colburn, T., Leggett, G. J.: Influence of solvent environment and tip chemistry on the contact mechanics of tip-sample interactions in friction force microscopy of self-assembled monolayers of mercaptoundecanoic Acid and dodecanethiol. *Langmuir* 2007, 23, 4959-64.
- [19] Frisbie, C. D., Rozsnyai, L. F., Noy, A., Wrighton, M. S., Lieber, C. M.: Functional Group Imaging by Chemical Force Microscopy. *Science* 1994, 265, 2071-2074.
- [20] Askwith, T. C.; Cameron, A.; Crouch, R. F. Chain Length of Additives in Relation to Lubricants in Thin Film and Boundary Lubrication. *Proc. R. Soc. London, Ser. A* 1966, 291, 500–519.

- 1
2
3
4
5
6
7
8
9
10
11
12
13
14
15
16
17
18
19
20
21
22
23
24
25
26
27
28
29
30
31
32
33
34
35
36
37
38
39
40
41
42
43
44
45
46
47
48
49
50
51
52
53
54
55
56
57
58
59
60
61
62
63
64
65
- [21] Crespo, A., Mazuyer, D., Morgado, N., Tonck, A., Georges, J-M., Cayer-Barrio, J.: Methodology to Characterize Rheology, Surface Forces and Friction of Confined Liquids at the Molecular Scale Using the ATLAS Apparatus. *Tribol. Lett.* 2017, 65, 138.
- [22] Georges, J-M., Millot, S., Loubet, J-L., Tonck, A.: Drainage of thin liquid films between relatively smooth surfaces. *J. Chem. Phys.* 1993, 98, 7345.
- [23] Tonck, A., Bec, S., Mazuyer, D., Georges, J-M., Lubrecht, A. A.: The École Centrale de Lyon surface force apparatus: An application overview. *Proc. Inst. Mech. Eng.* 1999, Part J 213, 353-361.
- [24] Crespo, A., Morgado, N., Mazuyer, D., Cayer-Barrio, J.: Effect of Unsaturation on the Adsorption and the Mechanical Behavior of Fatty Acid Layers. *Langmuir* 2018, 34, 15, 4560-4567.
- [25] Chen, Y-L., Israelachvili, J. N.: Effects of Ambient Conditions on Adsorbed Surfactant and Polymer Monolayers. *J. Phys. Chem.* 1992, 96, 7752-7760.
- [26] Georges, J-M., Tonck, A., Mazuyer, D.: Interfacial friction of wetted monolayers. *Wear* 1994, 175, 59-62.
- [27] Coulomb, C. A.: *Théorie des Machines Simples*, Gallica Bibliothèque Nationale de France, Paris, France (1821) (In French).
- [28] Jabbarzadeh, A., Harrowell, P., Tanner, R.I.: Crystal Bridge Formation Marks the Transition to Rigidity in a Thin Lubrication Film. *Phys. Rev. Lett.* 2006, 96, 206102.
- [29] Cui, S. T., Cummings, P. T., Cochran, H. D.: Molecular simulation of the transition from liquidlike to solidlike behavior in complex fluids confined to nanoscale gaps. *J. Chem. Phys.* 2001, 114, 7189.
- [30] Campen, S., Green, J. H., Lamb, G.D., Spikes, H.A.: In Situ Study of Model Organic Friction Modifiers Using Liquid Cell AFM; Saturated and Mono-unsaturated Carboxylic Acids. *Tribol. Lett.* 2015, 57, 18.

- 1
2
3
4
5
6
7
8
9
10
11
12
13
14
15
16
17
18
19
20
21
22
23
24
25
26
27
28
29
30
31
32
33
34
35
36
37
38
39
40
41
42
43
44
45
46
47
48
49
50
51
52
53
54
55
56
57
58
59
60
61
62
63
64
65
- [31] Wheeler, D.H., Potente, D., Wittcoff, H.: Adsorption of dimer, trimer, stearic, oleic, linoleic, nonanoic and azelaic acids on ferric oxide. *J. Am. Oil Chem. Soc.* 1971, 48, 125-128.
- [32] Mazuyer, D., Cayer-Barrioz, J., Tonck, A., Jarnias, F.: Friction Dynamics of Confined Weakly Adhering Boundary Layers. *Langmuir* 2008, 24, 3857-3866.
- [33] Mazuyer, D. Tonck, A., Cayer-Barrioz, J.: Friction control at the molecular level. In: *Superlubricity, Vol.1* (Eds: A. Erdemir, J-M. Martin), Elsevier BV, 2007, Ch. 22.
- [34] Greenwood, J. A., Williamson, J. B. P.: Contact between nominally flat surfaces. *Proc. Roy. Soc.* 1966, A295, 300-319.
- [35] Johner, A., Joanny, J-F.: Adsorption of polymeric brushes: Bridging. *J. Chem. Phys.* 1992, 96, 6257.
- [36] Joanny, J-F.: Lubrication by molten polymer brushes. *Langmuir* 1992, 8, 989-995.
- [37] Tabor, D.: The Role of Surface and Intermolecular Forces in Thin Film Lubrication. In: *Microscopic Aspects of Adhesion and Lubrication, Tribology Series 7*, Elsevier, ed. J. M. Georges, 1982, pp. 651-682.
- [38] Homola, A. M., Israelachvili, J. N., McGuiggan, P. M., Gee, M.L.: Fundamental experimental studies in tribology: The transition from “interfacial” friction of undamaged molecularly smooth surfaces to “normal” friction with wear. *Wear* 1990, 136, 1, 65-83.
- [39] Thomas, R. C., Houston, J. E., Crooks, R.M., Kim, T., Michalske, T. A.: Probing Adhesion Forces at the Molecular Scale. *J. Am. Chem. Soc.* 1995, 117, 3830-3834.
- [40] Archard, J.F.: Contact and Rubbing of Flat Surfaces. *Journal of Applied Physics* 1953, 24, 981-988.
- [41] Carpick, R., Salmeron, M.: Scratching the Surface: Fundamental Investigations of Tribology with Atomic Force Microscopy. *Chem. Rev.* 1997, 97, 1163-1194.